



Published in final edited form as:

Cancer Epidemiol Biomarkers Prev. 2023 April 03; 32(4): 542–549.

doi:10.1158/1055-9965.EPI-22-0941.

Methylation Signature Implicated in Immuno-Suppressive Activities in Tubo-Ovarian High-Grade Serous Carcinoma

Chen Wang¹, Matthew S. Block², Julie M. Cunningham³, Mark E. Sherman⁴, Bryan M. McCauley⁵, Sebastian M. Armasu⁵, Robert A. Vierkant¹, Nadia Traficante^{6,7}, Australian Ovarian Cancer Study Group^{6,8}, Aline Talhouk^{9,10}, Susan J. Ramus^{11,12}, Nadja Pejovic¹³, Martin Köbel¹⁴, Brooke D. Jorgensen¹⁵, Dale W. Garsed^{6,7}, Sian Fereday^{6,7}, Jennifer A. Doherty¹⁶, Dinuka Ariyaratne⁶, Michael S. Anglesio^{9,10,17}, Martin Widschwendter¹⁸, Tanja Pejovic^{19,20}, Jesus Gonzalez Bosquet²¹, David D. Bowtell^{6,7}, Stacey J. Winham¹, Ellen L. Goode¹⁵

¹Department of Quantitative Health Sciences, Division of Computational Biology, Mayo Clinic, Rochester, MN, USA.

²Department of Oncology, Mayo Clinic, Rochester, MN, USA.

³Department of Laboratory Medicine and Pathology, Mayo Clinic, Rochester, MN, USA.

⁴Department of Quantitative Health Sciences, Mayo Clinic, Jacksonville, FL, USA.

⁵Department of Quantitative Health Sciences, Division of Clinical Trials and Biostatistics, Mayo Clinic, Rochester, MN, USA.

⁶Peter MacCallum Cancer Centre, Melbourne, Victoria, Australia.

⁷Sir Peter MacCallum Department of Oncology, The University of Melbourne, Parkville, Victoria, Australia.

⁸Centre for Cancer Research, The Westmead Institute for Medical Research and Department of Gynaecological Oncology, Westmead Hospital, The University of Sydney, Sydney, New South Wales, Australia.

⁹British Columbia's Ovarian Cancer Research (OVCARE) Program, BC Cancer, Vancouver General Hospital, and University of British Columbia, Vancouver, BC, Canada.

¹⁰Department of Obstetrics and Gynecology, University of British Columbia, Vancouver, BC, Canada.

¹¹School of Clinical Medicine, Faculty of Medicine, University of NSW Sydney, Sydney, New South Wales, Australia.

¹²Adult Cancer Program, Lowy Cancer Research Centre, University of NSW Sydney, Sydney, New South Wales, Australia.

¹³St Louis School of Medicine, St. Louis, MO, USA.

Corresponding Author: Ellen L. Goode, Ph.D., M.P.H., Department of Quantitative Health Sciences, Mayo Clinic, 200 First Street SW, Rochester, MN 55905, USA, Phone 507/266-7997, egoode@mayo.edu.

The authors declare no potential conflicts of interest.

14. Department of Pathology and Laboratory Medicine, University of Calgary, Calgary, AB, Canada.
15. Department of Quantitative Health Sciences, Division of Epidemiology, Mayo Clinic, Rochester, MN, USA.
16. Huntsman Cancer Institute, Department of Population Health Sciences, University of Utah, Salt Lake City, UT, USA.
17. Department of Pathology and Laboratory Medicine, University of British Columbia, Vancouver, BC, Canada.
18. European Translational Oncology Prevention and Screening (EUTOPS) Institute, Universität Innsbruck, Hall in Tirol, Austria.
19. Department of Obstetrics and Gynecology, Oregon Health & Science University, Portland, OR, USA.
20. Knight Cancer Institute, Oregon Health & Science University, Portland, OR, USA.
21. Department of Obstetrics and Gynecologic, Division of Gynecologic Oncology, University of Iowa, Iowa City, IA, USA.

Abstract

Background: Better understanding of prognostic factors in tubo-ovarian high-grade serous carcinoma (HGSC) is critical, as diagnosis confers an aggressive disease course. Variation in tumor DNA methylation shows promise predicting outcome, yet prior studies were largely platform-specific and unable to evaluate multiple molecular features.

Methods: We analyzed genome-wide DNA methylation in 1,040 frozen HGSC, including 325 previously reported upon, seeking a multi-platform quantitative methylation signature which we evaluated in relation to clinical features, tumor characteristics, time to recurrence/death, extent of CD8⁺ tumor-infiltrating lymphocytes (TILs), gene expression molecular subtypes, and gene expression of the ATP-binding cassette transporter TAP1.

Results: Methylation signature was associated with shorter time to recurrence, independent of clinical factors (N=715 new set, HR 1.65, 95% CI 1.10–2.46, p=0.015; N=325 published set HR 2.87, 95% CI 2.17–3.81, p=2.2 × 10⁻¹³) and remained prognostic after adjustment for gene expression molecular subtype and TAP1 expression (N=599, HR 2.22, 95% CI 1.66–2.95, p=4.1 × 10⁻⁸). Methylation signature was inversely related to CD8⁺ TIL levels (p=2.4 × 10⁻⁷) and TAP1 expression (p=0.0011) and was associated with gene expression molecular subtype (p=5.9 × 10⁻⁴) in covariate-adjusted analysis.

Conclusions: Multi-center analysis identified a novel quantitative tumor methylation signature of HGSC applicable to numerous commercially available platforms indicative of shorter time to recurrence/death, adjusting for other factors. Along with immune cell composition analysis, these results suggest a role for DNA methylation in the immunosuppressive microenvironment.

Impact: This work aids in identification of targetable epigenome processes and stratification of patients for whom tailored treatment may be most beneficial.

Keywords

ovarian cancer; prognosis association; meta-analysis; epigenomics; tumor immune microenvironment

INTRODUCTION

Tube-ovarian high-grade serous carcinoma (HGSC) is the most common histotype of epithelial ovarian cancer (1). The existence of HGSC subtypes based on epigenome-wide tumor DNA methylation patterns has been demonstrated in several studies (2, 3) and provides potential avenues for risk prediction and novel therapeutics (4, 5). Based on semi-supervised clustering analysis of DNA methylation at 450,000 CpG sites in 337 HGSCs, we reported a signature based on 60 CpG loci that predicted time to disease recurrence (6). Women with tumors of the more unfavorable methylation-based subtype (termed “L class” in prior report) had median time to recurrence 1.2 years shorter than other patients (“R class”; $p = 2.9 \times 10^{-3}$) after adjusting for clinical covariates. The poor prognosis signatures showed increased methylation of chromosome 6p21.3 genes enriched for immune response processes, including TAP1, an ATP-binding cassette transporter. TAP1 methylation correlated with lower TAP1 RNA expression, reduced CD8⁺ tumor-infiltrating lymphocytes (TILs), and altered genome-wide regulation of immune-related genes (6). Subsequent RNA expression analysis of over 3,500 archival tumors (including 21 from the initial methylation study (6)), found that increased TAP1 RNA expression was associated with longer HGSC overall survival time ($p=8.3 \times 10^{-18}$, adjusted for covariates) (7).

To better understand the complex, potentially prognostic interplay of tumor DNA methylation signatures, immune features, and previously reported gene expression molecular subtypes (8), we undertook a novel multi-site investigation that sought to overcome two methodological limitations of the original predictor (6): 1) study- and platform-dependence which may limit generalizability, and 2) dichotomization which may misrepresent a continuum of epigenomics-implicated prognostic risk. Here, we describe a quantitative scoring strategy applicable to a variety of commercially available DNA methylation platforms which we applied to data from nearly 800 additional HGSC patients from multiple independent collections. In subset analyses, we examined several tumor-based immune and microenvironment factors, including TAP1 gene expression, extent of CD8⁺ TILs, and gene expression molecular subtypes. Better understanding of prognostic factors is of prime importance, as diagnoses of HGSC continue to confer an aggressive disease course.

MATERIALS AND METHODS

Study Participants and DNA Methylation Data

We analyzed HGSC studies with Illumina Infinium BeadChip methylation data derived from fresh frozen tumor samples: TCGA (3), AOCS (9), and studies from University College London (UCL) (10), Oregon Health Sciences University (OHSU) (11), and UIHC (12) (Supplementary Table 1). Methylation assays and quality control (QC) methods for each study have been described elsewhere (3, 10–13); OHSU data were subjected to previously

applied QC procedures (6). In addition, we report outcomes for an additional seven years of follow-up for 325 previously reported Mayo Clinic patients (6), resulting in 71 additional events, excluding non-HGSCs revealed upon detailed IHC-supported pathologic review (14). Time to disease recurrence or progression was defined by each study (3, 6, 9–12), and, where recurrence/progression was unavailable, death from any cause was utilized (Supplementary Table 1). We excluded participants with missing data on age at diagnosis, extent of residual disease following primary debulking surgery, or time to recurrence/death.

Methylation Signature

A tumor methylation signature for each participant was defined based on a previously described Illumina Infinium HumanMethylation450 BeadChip training set (N=198 Mayo Clinic study participants, a subset of those included here) (6). Based on elastic-net regularized generalized linear models (glmnet) (15, 16), quantitative methods were used to identify the most informative CpG sites and construct a methylation signature applicable to a variety of methylation platforms (Supplementary Methods 1, Supplementary Table 2, Supplementary Table 3). This resulted in an approximated tumor methylation signature for TCGA, AOCS, UCL, OHSU, and UIHC participants, the tumors of which were measured on either the Illumina Infinium HumanMethylation27 or the Illumina Infinium MethylationEPIC BeadChip. Substantial concordance of methylation signatures was achieved across platforms (correlation coefficient range, 0.85 to 0.98; $p < 1 \times 10^{-16}$), as shown in Supplementary Figure 1. Tumor methylation signatures were not re-estimated for Mayo Clinic participants in the prior testing set (6). Each HGSC was assigned a quantitative methylation signature ranging from -1 to 1; higher scores were consistent with the previously termed the “L class” poorer prognosis signature (6). The interquartile range of the score is 0.53 and the standard deviation is 0.34. Additional detail is provided in Supplementary Methods 1, Supplementary Table 2, Supplementary Table 3.

Clinical and Prognosis Associations

We evaluated the association between study site and the following clinical factors using Pearson’s chi-square test for categorical factors and ANOVA for continuous measures: age at diagnosis (continuous), extent of residual disease following primary debulking surgery (optimal debulking <1 cm remaining, sub-optimal debulking ≥ 1 cm remaining), disease stage (early, advanced), and germline pathogenic *BRCA1/2* mutation status based on clinical records and/or research-based DNA sequencing (*BRCA1* mutation carrier, *BRCA2* mutation carrier, tested non-carrier) (17). We also assessed the association between continuous methylation signatures and the same clinical factors using ANOVA for categorical measures and Spearman correlation for continuous measures. Analyses were conducted separately for each study and meta-analyzed. Study-specific Cox regressions considered time to recurrence, defined as time from diagnosis to evidence of first disease recurrence/progression or death, and used methylation signature as a continuous measure, adjusting for age at diagnosis, and surgical debulking outcome (optimal, sub-optimal); stage (early, advanced, unknown) was an additional covariate in Mayo Clinic and TCGA only, as the other studies had no or few patients with early stage HGSC (Supplementary Table 1). We accounted for left truncation and censored at 10 years from diagnosis and combined resulting HR estimates across studies using random effects meta-analysis

where appropriate. Random effects meta-analysis was performed using restricted maximum likelihood (REML) as implemented using the R package ‘metafor’ and the ‘RMA’ function. Tests for heterogeneity by study used interaction term likelihood ratio testing. We also conducted full sets of analyses excluding Mayo Clinic participant data that were reported on previously (6), even though additional follow-up time was observed. In 320 Mayo Clinic participants with detailed information of sample collection data, we tested whether methylation signature scores had statistically significant differences for omental-sourced specimens (N=66; 20%) versus samples from other tissue sources (N=254; 80%) using a two sample t-test, to examine whether omental tissue sites may be associated with molecular differences as previously reported (8).

Molecular Data

Where available on subsets of participants, we examined the following tumor-based data in relation to methylation signature: gene expression molecular subtype (C1.MES, C2.IMM, differentiated [C4.DIFF], C5.PRO; N=746) (8), tumor RNA expression of TAP1 (N=605) (3, 7), and levels of CD8⁺ TILs based on counts per 400x magnification field (negative [no TILs], low [1–2 TILs], moderate [3–19 TILs], high [>20 TILs]; N=222) (18). Gene expression molecular subtype and tumor RNA expression of TAP1 were available on an overlapping set of N=599 participants. Key resources are available upon request. Univariate association testing between these factors and methylation signature used Spearman correlation for continuous variables (e.g., TAP1 expression) and ANOVA for categorical variables (e.g., CD8⁺ TILs and gene expression molecular subtype); multivariate testing adjusting for age, stage, study site, and debulking status utilized linear regression. We also conducted analysis of methylation signature and time to recurrence/death in case strata defined by gene expression molecular subtype. Multivariate Cox regression of these factors and methylation signature in relation to time to disease recurrence was adjusted for age, stage, study site, and debulking status. As above, we conducted full sets of analyses excluding Mayo Clinic participants that were included in our prior publication (6).

PanImmune Features

With TCGA data, we evaluated “PanImmune features”, as previously described for 33 TCGA cancer types, including HGSC (19). Briefly, these PanImmune features were composed of *in-silico* deconvolution estimations of cellular compositions (e.g., “Leukocyte Fraction” and “Stromal Fraction”), genetic and genomic alteration burden scores as total number or summarized rate of corresponding somatic changes (e.g., “SNV Neoantigens” and “Silent Mutation Rate”), and collective ‘omic inference about biological processes/ pathway activities (e.g., “TGF-beta Response” and “IFN-gamma Response”). Analyses estimated Spearman rank correlations between methylation signature and these PanImmune features correcting for multiple testing.

Cis Association between Individual CpGs and TAP1 mRNA Expression

We selected CpG loci within 3 kb distances of TAP1 gene region for cis-association evaluations, and further excluded CpGs at the same location with a single nucleotide polymorphism, determined to be cross-reactive, or overlapped genetic variants. We assessed the correlation between gene expression and CpG beta values using a one-sided Spearman

rank correlation test for negative associations in Mayo Clinic (N=312) and AOCS (N=33) with Illumina Infinium HumanMethylation450 BeadChip data, as well as TCGA (N=260) with Illumina Infinium HumanMethylation27 BeadChips.

Data Availability

TCGA methylation data are available via the cBioPortal for Cancer Genomics (<https://www.cbioportal.org/>; RRID:SCR_014555). Other data are available on Gene Expression Omnibus (GEO; RRID:SCR_005012) under the following accession numbers: GSE65820 and GSE211686 (AOCS), GSE72021 (UCL), GSE133556 (UIHC), and GSE223467 (Mayo Clinic, OHSU).

RESULTS

Characteristics of Study Participants and Baseline Clinical Features

The analysis included 1,040 HGSC patients from six studies with an average age at diagnosis of 60.8 years; 95% of patients were diagnosed at advanced stage, 72% were debulked with <1 cm remaining, and 82.7% experienced disease recurrence or death within 10 years. Clinical characteristics are summarized by study in Supplementary Table 1 and showed minimal differences in survival or clinical features between newly analyzed and previously analyzed cases or by Illumina Infinium BeadChip platform (p-values>0.05), although percent of HGSCs with debulking to <1 cm remaining varied by study site (p<0.001), Australian Ovarian Cancer Study (AOCS) cases had more mesenchymal gene expression molecular subtype (C1.MES) tumors (p<0.001), and age at diagnosis differed slightly (p=0.01). Median overall survival estimates ranged from 1.89 years to 3.96 years per study, with those focused on chemo-resistant or advanced disease (e.g., AOCS, the University of Iowa Hospitals and Clinics [UIHC] study) showing, as expected, the shortest survival times. Approximately 95% of cases were of self-reported European ancestry. To enable replication of original methylation subtype finding which was derived from semi-supervised clustering approach with requirements for complete clinical covariates and conditional on only one 450K platform, a quantitative method was developed to generalize study- and platform-independent methylation signature scoring based on Mayo training set and evaluated in Mayo testing set (details seen in Supplementary Methods 1). Estimation of the quantitative methylation signature score was done to approximate the original methylation subtype score. The concordance between the original and newly derived scores was evaluated to confirm that they had the expected strong positive relationship (Supplementary Figure 1). Methylation signature was not associated with age, stage, debulking status, or germline pathogenic *BRCA1/2* mutation status, in any study or overall (p-values > 0.05; Supplementary Figure 2). There was no association between methylation signature and tissue source (omentum v other: p-value > 0.05).

Time-to-Recurrence Analyses

Study-specific, covariate-adjusted Cox regression analyses revealed methylation score hazard ratio point estimates consistently greater than one in association analyses of methylation signature with time to disease recurrence or death. Random effects meta-analysis was used to combine covariate-adjusted study-specific results. Overall, we found

that each unit increase in methylation signature was associated with a 95% increase in risk of disease recurrence or death (N=1,040, HR 1.95, 95% CI 1.31–2.89, $p=0.0010$, Figure 1); however, heterogeneity of HRs was observed across study sites (heterogeneity $p=0.0062$). Results were consistent after exclusion of previously reported data (6) (N=715, new set HR 1.65, 95% CI 1.10–2.46, $p=0.0154$, heterogeneity $p=0.21$; N=325 published set HR 2.87, 95% CI 2.17–3.81, $p=2.19 \times 10^{-13}$, Figure 1). We examined whether methylation-associated risk was more pronounced or only apparent in cases with generally long survival time or those who survived more than five years; we found no evidence of time-dependent risks, having examined proportionality of hazards.

Evaluation of Immune Factors

In cross-sectional analyses, higher methylation signature values were found in tumors with no CD8⁺ TILs per high powered field or with a low/moderate CD8⁺ TIL level, compared to those with high CD8⁺ TIL levels (N=222; $p=5.7 \times 10^{-12}$ and 1.1×10^{-4} , respectively; Figure 2A). Results were consistent using four categories of CD8⁺ TILs and excluding data from cases published in the earlier methylation report (6). These results suggest differential methylation in the tumor-immune microenvironment. As observed previously in Mayo Clinic cases (6), *TAP1* gene expression differed by methylation signature; here, in a total of 605 cases (N=260 The Cancer Genome Atlas [TCGA], N=312 Mayo, N=33 AOCS) mRNA levels negatively correlated with methylation signature ($\rho=-0.45$, -0.60 , and -0.58 for TCGA, Mayo Clinic, and AOCS, respectively; p -values <0.05 ; Figure 2B). In 370 TCGA HGSC cases where extensive immune characterization has been conducted (19), methylation signature was negatively correlated with several immune features, including “Macrophage Regulation” and “Lymphocyte Infiltration Signature Score” (Figure 2C, Supplementary Figure 3). We further examined local correlation between individual CpG sites and *TAP1* mRNA expression in these datasets and found inverse relationships between beta values and expression levels. Association between CpGs was seen in suspected *TAP1* promoter regions in the Mayo Clinic data, many of which were also apparent in the smaller AOCS data (N=33); negative coefficients were also seen in the sparse TCGA data with only three interrogated CpG sites although associations were not statistically significant (Supplementary Figure 4).

Methylation Signature in Relationship to Gene Expression Molecular Subtype

We observed an association between methylation signature and gene expression molecular subtype characterized by mRNA profiling in TCGA, Mayo Clinic, and AOCS data such that immunoreactive (C2.IMM) subtype tumors had the lowest methylation signature values and proliferative (C5.PRO) subtype had the highest in each study (Figure 3A). This is consistent with our observed immune factor associations.

Multivariate Analyses of Methylation Signature

In 599 cases with gene expression molecular subtype and *TAP1* RNA expression data, we evaluated clinical and tumor factors that associated with methylation signature in a multivariate manner (Supplementary Table 4; Figure 3B). Considering age at diagnosis, stage, debulking status, study site, *TAP1* RNA expression, and gene expression molecular subtype, only age at diagnosis, *TAP1* RNA expression, and gene expression molecular

subtype were associated with methylation signature (p-values 0.017, 4.69×10^{-19} , and 1.24×10^{-9} , respectively; adjusted R-squared 0.30; Supplementary Table 4; Figure 3B). Similar results were seen among 423 cases with germline *BRCA1/2* mutation data; *BRCA1/2* mutation status did not associate with methylation signature. In a subset of 191 cases from Mayo Clinic and AOCS with CD8⁺ TIL data, multivariate modelling suggested that CD8⁺ TILs, TAP1 RNA expression, and gene expression molecular subtype independently contribute to prediction of methylation signature scores with an adjusted R² of 0.35 (Supplementary Table 4; Figure 3B). As multiple yet independent factors appear associated with methylation signature (TAP1 expression, gene expression molecular subtype, and CD8⁺ TIL levels), we do not expect methylation signature to be a simple surrogate for any of these tumor features.

Multivariate Analyses of Disease Outcome

Multivariate survival analysis of 599 participants with gene expression molecular subtype and TAP1 RNA expression data suggest that disease stage, surgical debulking status, and methylation signature were associated with time to recurrence/death at $p < 0.05$ with adjustment for age at diagnosis, study site (TCGA, Mayo Clinic, AOCS), TAP1 RNA expression, and gene expression molecular subtype (20, 21) (Table 1). Results suggest that each unit of methylation signature confers a more than two-fold increase in risk of recurrence/death (HR 2.22, 95% CI 1.66–2.95 $p = 4.46 \times 10^{-8}$). Compared to models examining association between methylation signature and time to recurrence/death that adjusted only for age (Table 1), results were similar (HR 2.19, 95% CI 1.74–2.76 $p = 3.83 \times 10^{-11}$) suggesting a stability in risk estimates regardless of these covariates. Sensitivity analyses excluding data from published cases (52%) eliminated a suggestion of association between methylation signature and time to recurrence/death in multivariate analyses (HR 0.98, 95% CI 0.58–1.66 $p = 0.94$); stage and study site (AOCS, TCGA) were predictors of outcome (Supplementary Table 5). To examine the role of CD8⁺ TIL levels, analyses were also restricted to 191 participants from two studies with IHC-based CD8⁺ TIL levels and *BRCA1/2* germline mutation data (Mayo Clinic, AOCS). Although inclusion of CD8⁺ TIL levels attenuated the methylation signature HR estimate from 2.21 to 1.90, methylation signature remained significantly associated with time to recurrence/death ($p = 0.009$, Supplementary Table 6). Stage and debulking status were also associated with time to recurrence/death in multivariate models ($p < 0.05$), while age, study site, germline *BRCA1/2* mutation status, TAP1 RNA expression, gene expression molecular subtype, and CD8⁺ TIL levels were significantly associated with time to recurrence/death ($p > 0.05$, Supplementary Table 6).

DISCUSSION

Using a novel tumor DNA methylation signature scoring scheme applicable to a variety of Illumina platforms, we report a novel analysis of over 1,000 women with HGSC. We affirm the prognostic value of a previously reported methylation signature, which was associated with time to disease recurrence or death and features of the immune microenvironment. Analysis of almost 700 additional cases demonstrated that increasing methylation signature scores were associated with up to a 65% increased risk of disease recurrence (HR 1.65,

95% CI 1.10–2.46) with adjustment for clinical covariates; similarly, in an updated analysis of more than 300 previously reported HGSCs with extended follow-up, the prognostic result was confirmed (HR 2.87, 95% CI 2.17–3.81). Our findings are consistent with a report on formalin-fixed paraffin-embedded tissue from 76 serous ovarian cancers, which found that hypermethylation at 6p21.3 CpG sites were associated with higher risk of mortality (HRs ranged from 3.10 to 5.25) (2). Here, HGSCs with higher methylation signature values showed decreased TAP1 mRNA expression, fewer CD8⁺ TILs, and under-representation of C2.IMM HGSCs. Accounting for these tumor characteristics as well as clinical factors, methylation signature scores remained significantly associated with time to disease recurrence or death.

Given associations between DNA methylation patterns and immune markers, we propose that mechanistic follow-up studies are needed to understand the role of epigenetic alterations in down-regulation of immune responses (5). Specifically, several epigenetically silenced genes residing on 6p21.3 are important in immune recognition and antigen presentation, (e.g., *TAP1* [a key prognostic gene] (7), *PSMB8*, *PSMB9*, *HLA-DQB1*, *HLA-DQB2*, *HLA-DMA*, and *HLA-DOA*). Epigenetically silenced chemokines in tumor cells can be reactivated by Decitabine (22). As TAP1 mRNA expression, gene expression molecular subtype, and CD8⁺ TIL levels are not associated with time to disease recurrence/death at $p < 0.05$ after adjustment for methylation signature scores in the full dataset, we hypothesize that methylation underlies the relationship of these factors with HGSC outcome. Although exclusion of published data removed the multivariate association between methylation signature at time to recurrence, it is possible that the DNA methylation signature is representative of a yet unknown mechanism, potentially related to epigenomic regulation of antigen presentation machinery.

There are several noteworthy strengths of this analysis. First, an approximation of a published semi-supervised method to a variety of Illumina Infinium BeadChips provided a quantitative methylation measure of broader utility. Second, the use of multiple study sites with robust fresh frozen tissues provided evaluation of replication of results. Throughout, we observed consistent evidence for associations with outcome and with tumor molecular features across studies, even though studies differed by geographic site/clinical practice, amount of follow-up time, and Illumina Infinium BeadChip used. Third, we performed sensitivity analyses, excluding previously reported results. Fourth, a large amount of overlaying molecular data across multiple studies provided an opportunity to gain novel insight into epigenetic and immune relationships. Nonetheless, our study has notable limitations as well. These include absence of racial and ethnic diversity, smaller sample sizes for analysis of tumor molecular features, and lack of examination of common inherited variation or lifestyle risk factors. Critical future work includes extensions into other populations, including women of African ancestry, a group thought to mount less potent anti-tumor immune responses against several cancers (23). In addition, future epidemiologic analyses of methylation signature should more broadly consider overall evidence of homologous recombination (not merely germline pathogenic *BRCA1/2* mutations), as well as polygenic risk scores and potentially modifiable lifestyle HGSC risk factors. This work also underscores the need for mechanistic investigation of methylation signatures, particularly focused on tumor immune features, cellular composition, and changes over

time (e.g., selection of pre-existing tumor cells with the signature). The development and validation of advanced laboratory methods to spatially profile DNA methylation at a cellular resolution will facilitate future methylation signature research (24, 25).

With additional research follow-up, a number of clinical advances could be enabled by these results. First, improved prognosis prediction especially with objective molecular measurements will facilitate clinical consultation with patients and the decision-making process for planning treatment if a real-time clinical test were available. Methylation-based assays are likely to be more technically amenable to measurement due greater expected biospecimen stability over RNA-based predictors; such a predictor could complement current DNA-based predictors of survival such as homologous recombination and CCNE1 amplification. Second, as a biomarker reflective of tumor epigenetic status, the methylation signature could be used in clinical trials to correlate with outcomes and stratify patients. Third, this work sheds light on avenues of mechanistic studies to identify underlying dysregulated pathways for each methylation signature and ultimately advance more personalized therapies for HGSC patients. In summary, our observation that a HGSC methylation signature associates with disease outcome and a suite of tumor immune features provides a novel, important framework for avenues of subsequent tumor methylation-based HGSC research.

Supplementary Material

Refer to Web version on PubMed Central for supplementary material.

ACKNOWLEDGMENTS

AOCS: The Australian Ovarian Cancer Study gratefully acknowledges additional support from Ovarian Cancer Australia and the Peter MacCallum Foundation. The AOCS also acknowledges the cooperation of the participating institutions in Australia and acknowledges the contribution of the study nurses, research assistants and all clinical and scientific collaborators to the study. The complete AOCS Study Group can be found at www.aocstudy.org. We would like to thank all the women who participated in these research programs. We gratefully acknowledge the Departments of Gynaecological Oncology, Medical Oncology and Anatomical Pathology at Westmead Hospital, Sydney. The Australian Ovarian Cancer Study Group was supported by the U.S. Army Medical Research and Materiel Command under DAMD17-01-1-0729, The Cancer Council Victoria, Queensland Cancer Fund, The Cancer Council New South Wales, The Cancer Council South Australia, The Cancer Council Tasmania, and The Cancer Foundation of Western Australia (Multi-State Applications 191, 211, and 182) and the National Health and Medical Research Council of Australia (NHMRC; ID199600; ID400413, and ID400281). The Australian Ovarian Cancer Study gratefully acknowledges additional support from Ovarian Cancer Australia and the Peter MacCallum Foundation. The Gynaecological Oncology Biobank at Westmead (GynBiobank), a member of the Australasian Biospecimen Network-Oncology group, was funded by the National Health and Medical Research Council of Australia (ID 310670 & ID 628903) and the Cancer Institute NSW (12/RIG/1-17 & 15/RIG/1-16). D.W. Garsed is supported by NHMRC Ideas Grant (APP1186505). D.D.L. Bowtell is supported by a National Health and Medical Research Council (NHMRC) Fellowship (APP1117044) and Program Grant (APP1092856). OHSU: Sherie Hildreth Ovarian Cancer (SHOC) Foundation. UCL: European Union's Horizon 2020 European Research Council Programme, H2020 BRCA-ERC under Grant Agreement No. 742432. Other Data: National Institutes of Health/National Cancer Institute (NCI) Grant R01-CA172404.

Financial Support:

E.L. Goode was supported by the National Cancer Institute (P50-CA136393, R01-CA248288, P30-CA015083).

REFERENCES

1. Bowtell DD, Bohm S, Ahmed AA, Aspuria PJ, Bast RC Jr., Beral V, et al. Rethinking ovarian cancer II: reducing mortality from high-grade serous ovarian cancer. *Nat Rev Cancer*. 2015;15:668–79. [PubMed: 26493647]
2. Bodelon C, Killian JK, Sampson JN, Anderson WF, Matsuno R, Brinton LA, et al. Molecular classification of epithelial ovarian cancer based on methylation profiling: evidence for survival heterogeneity. *Clin Cancer Res*. 2019;25:5937–46. [PubMed: 31142506]
3. Cancer Genome Atlas Research Network. Integrated genomic analyses of ovarian carcinoma. *Nature*. 2011;474:609–15. [PubMed: 21720365]
4. Reid BM, Fridley BL. DNA methylation in ovarian cancer susceptibility. *Cancers (Basel)*. 2020;13. [PubMed: 33375062]
5. Ishak CA, Lheureux S, De Carvalho DD. DNA methylation as a robust classifier of epithelial ovarian cancer. *Clin Cancer Res*. 2019;25:5729–31. [PubMed: 31337645]
6. Wang C, Cicek MS, Charbonneau B, Kalli KR, Armasu SM, Larson MC, et al. Tumor hypomethylation at 6p21.3 associates with longer time to recurrence of high-grade serous epithelial ovarian cancer. *Cancer Res*. 2014;74:3084–91. [PubMed: 24728075]
7. Millstein J, Budden T, Goode EL, Anglesio MS, Talhouk A, Intermaggio MP, et al. Prognostic gene expression signature for high-grade serous ovarian cancer. *Ann Oncol*. 2020;31:1240–50. [PubMed: 32473302]
8. Talhouk A, George J, Wang C, Budden T, Tan TZ, Chiu DS, et al. Development and validation of the gene expression predictor of high-grade serous ovarian carcinoma molecular subtype (PrOTYPE). *Clin Cancer Res*. 2020;26:5411–23. [PubMed: 32554541]
9. Patch AM, Christie EL, Etemadmoghadam D, Garsed DW, George J, Fereday S, et al. Whole-genome characterization of chemoresistant ovarian cancer. *Nature*. 2015;521:489–94. [PubMed: 26017449]
10. Bartlett TE, Jones A, Goode EL, Fridley BL, Cunningham JM, Berns EM, et al. Intra-gene DNA methylation variability is a clinically independent prognostic marker in women’s cancers. *PLoS One*. 2015;10:e0143178. [PubMed: 26629914]
11. Pejovic T, Pande NT, Mori M, Mhawech-Fauceglia P, Harrington C, Mongoue-Tchokote S, et al. Expression profiling of the ovarian surface kinome reveals candidate genes for early neoplastic changes. *Transl Oncol*. 2009;2:341–9. [PubMed: 19956396]
12. Reyes HD, Devor EJ, Warrier A, Newton AM, Mattson J, Wagner V, et al. Differential DNA methylation in high-grade serous ovarian cancer (HGSOC) is associated with tumor behavior. *Sci Rep*. 2019;9:17996. [PubMed: 31784612]
13. Kommoss S, Winterhoff B, Oberg A, Konecny GE, Wang C, Riska SM, et al. Bevacizumab may differentially improve ovarian cancer outcome in patients with proliferative and mesenchymal molecular subtypes. *Clin Cancer Res*. 2017;23(14):3794–3801. [PubMed: 28159814]
14. Kobel M, Rahimi K, Rambau PF, Naugler C, Le Page C, Meunier L, et al. An immunohistochemical algorithm for ovarian carcinoma typing. *Int J Gynecol Pathol*. 2016;35:430–41. [PubMed: 26974996]
15. Friedman J, Hastie T, Tibshirani R. Regularization paths for generalized linear models via coordinate descent. *J Stat Softw*. 2010;33:1–22. [PubMed: 20808728]
16. Zou HH, Trevor. Regularization and variable selection via the elastic net. *Journal of the Royal Statistical Society, Series B*. 2005;67:301–20.
17. Cunningham JM, Cicek MS, Larson NB, Davila J, Wang C, Larson MC, et al. Clinical characteristics of ovarian cancer classified by BRCA1, BRCA2, and RAD51C status. *Sci Rep*. 2014;4:4026. [PubMed: 24504028]
18. Ovarian Tumor Tissue Analysis Consortium, Goode EL, Block MS, Kalli KR, Vierkant RA, Chen W, et al. Dose-response association of CD8+ tumor-infiltrating lymphocytes and survival time in high-grade serous ovarian cancer. *JAMA Oncol*. 2017;3:e173290. [PubMed: 29049607]
19. Thorsson V, Gibbs DL, Brown SD, Wolf D, Bortone DS, Ou Yang TH, et al. The immune landscape of cancer. *Immunity*. 2018;48:812–30 e14. [PubMed: 29628290]

20. Wang C, Armasu SM, Kalli KR, Maurer MJ, Heinzen EP, Keeney GL, et al. Pooled clustering of high-grade serous ovarian cancer gene expression leads to novel consensus subtypes associated with survival and surgical outcomes. *Clin Cancer Res.* 2017;23:4077–85. [PubMed: 28280090]
21. Konecny GE, Wang C, Hamidi H, Winterhoff B, Kalli KR, Dering J, et al. Prognostic and therapeutic relevance of molecular subtypes in high-grade serous ovarian cancer. *J Natl Cancer Inst.* 2014;106.
22. Dangaj D, Bruand M, Grimm AJ, Ronet C, Barras D, Duttagupta PA, et al. Cooperation between constitutive and inducible chemokines enables T cell engraftment and immune attack in solid tumors. *Cancer Cell.* 2019;35:885–900 e10. [PubMed: 31185212]
23. Ozdemir BC, Dotto GP. Racial differences in cancer susceptibility and survival: more than the color of the skin? *Trends Cancer.* 2017;3:181–97. [PubMed: 28718431]
24. Moss J, Magenheim J, Neiman D, Zemmour H, Loyfer N, Korach A, et al. Comprehensive human cell-type methylation atlas reveals origins of circulating cell-free DNA in health and disease. *Nat Commun.* 2018;9:5068. [PubMed: 30498206]
25. Zheng H, Momeni A, Cedoz PL, Vogel H, Gevaert O. Whole slide images reflect DNA methylation patterns of human tumors. *NPJ Genom Med.* 2020;5:11. [PubMed: 32194984]

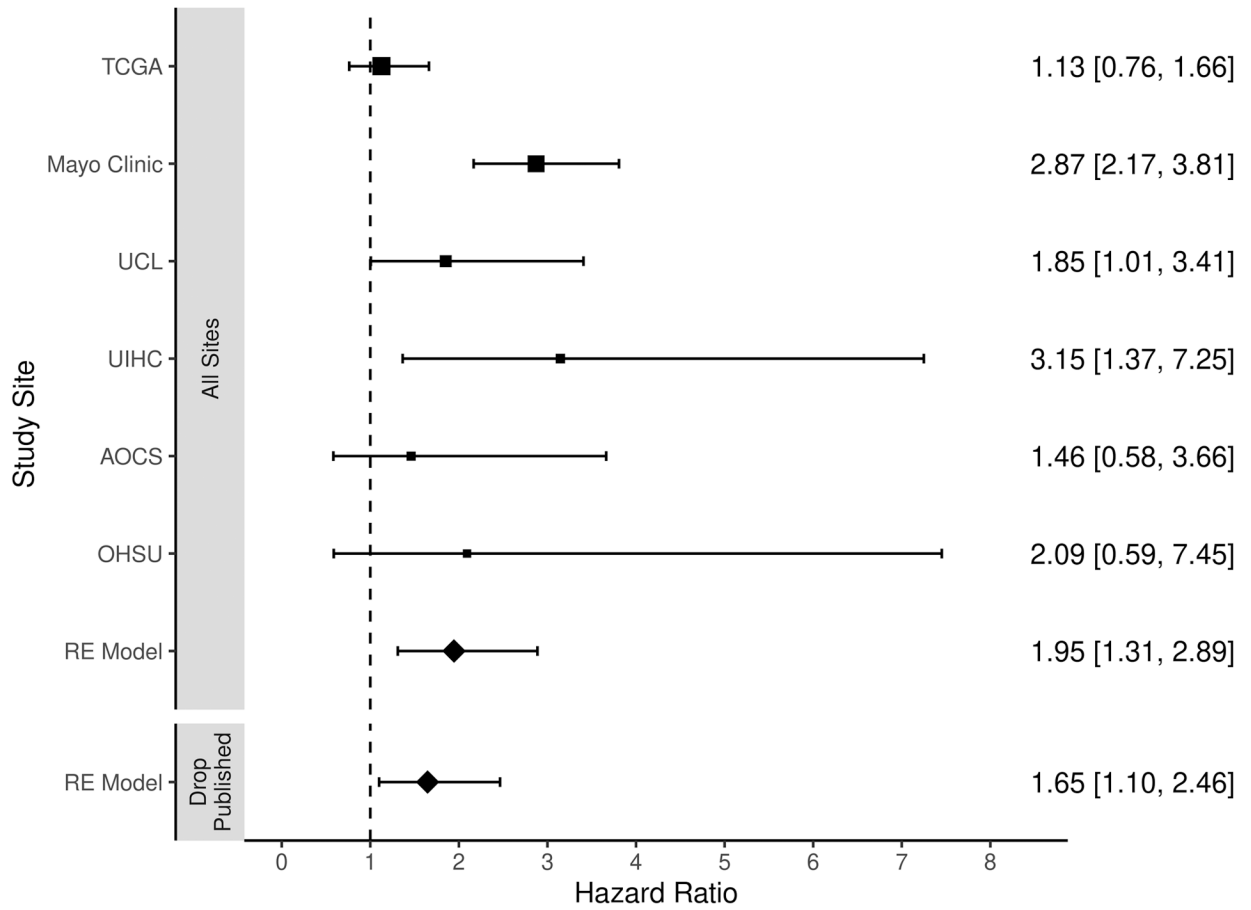


Figure 1. Associations with Time to Disease Recurrence by Study and Combined Mayo Clinic; TCGA, The Cancer Genome Atlas; AOCS, Australian Ovarian Cancer Study; OHSU, Oregon Health Sciences University UCL, University of College London; UIUC, University of Iowa Hospitals and Clinics; hazard ratios and 95% confidence intervals for methylation signature and time to disease recurrence or death in each study adjusted for age at diagnosis, debulking status (optimal, sub-optimal), and, for TCGA and Mayo Clinic, stage (early, advanced); RE Model represents all cases N=1,040; RE Model Drop Published represents non-Mayo cases N=715; dotted vertical line at 1.0 represents a hazard ratios equal to one (no association).

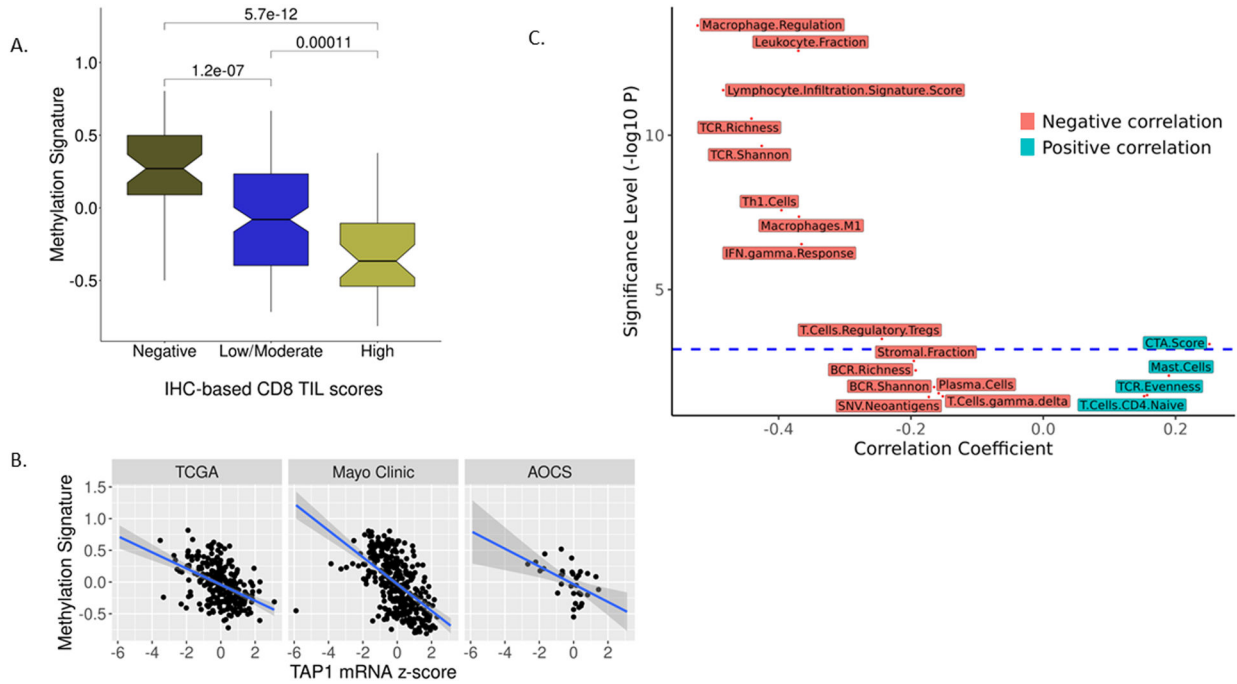


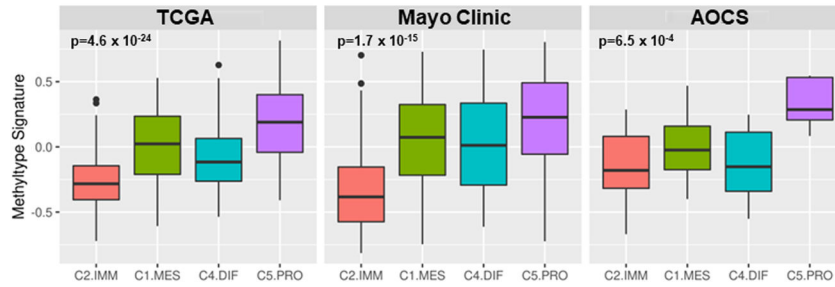
Figure 2. Methylation Signature and Immune Factors

A. Boxplots of methylation signature scores with respect to CD8⁺ tumor-Infiltrating lymphocytes (TILs). N=191 cases from Mayo Clinic, N=14 cases from AOCS, and N=17 cases from OHSU. Levels of CD8⁺ TILs per high powered field: none, low-moderate [1–19 CD8⁺ TILs], high [>20 CD8⁺ TILs] ascertained by immunohistochemistry (18).

B. Scatterplots between methylation signature scores and TAP1 mRNA expression level (z-score) in three studies. N=260 cases from TCGA, N=312 cases from Mayo Clinic, and N=33 cases from AOCS.

C. Volcano plot shows methylation signature correlations with omics-inferred immune activities in 370 TCGA cases; x-axis is correlation coefficient and y-axis are statistical significance defined as $-\log_{10}(\text{p-value})$. On the upper left are immune activities most negatively correlated with methylation signature. The dashed line denotes the significance level based on a Bonferroni correction for 58 comparisons.

A.



B.

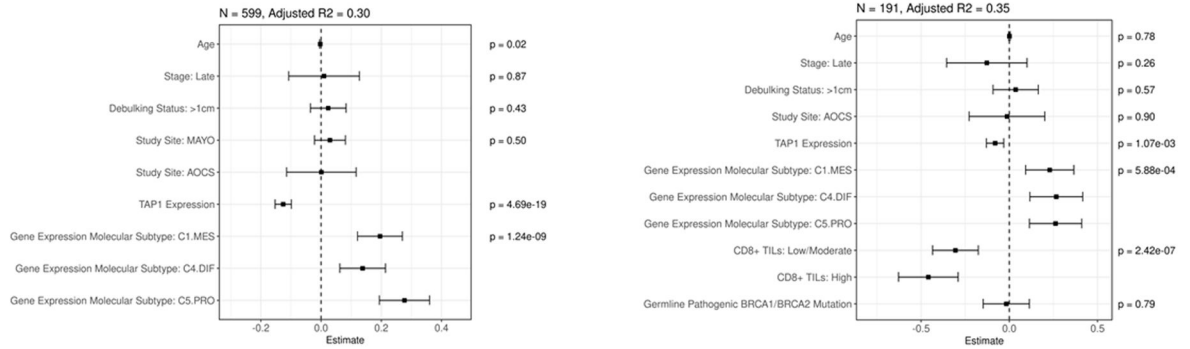


Figure 3. Methylation Signature, Microenvironment Indicators, and Multivariate Analysis

A. Methylation signature score had significant associations with gene expression molecular subtypes characterized by tumor transcriptome. TCGA, N=371; Mayo Clinic N=309; AOCs, N=66.

B. Coefficient estimates from multivariate modeling of methylation signature using linear regression in cases with gene expression data. Left: TCGA, AOCs, Mayo Clinic (N=599). Right: AOCs, Mayo Clinic with additional CD8⁺ TIL and BRCA1/2 mutation data (N=191). Models include age at diagnosis, stage (early as referent), debulking status (optimal debulking as referent), study site (Mayo Clinic as referent), TAP1 RNA expression, gene expression molecular subtype (C2.IMM as referent). Right models also include CD8⁺ TIL level (no CD8⁺ TILs as referent) and germline pathogenic *BRCA1/2* mutation (tested non-carrier as referent). Adjusted R-squared estimates and likelihood-ratio testing p-values shown.

TABLE 1.
Associations of Time to Recurrence/Death Among Studies with Gene Expression Data

	Age-Adjusted			Multivariate		
	N	HR (95% CI)	p-value	HR (95% CI)	p-value	
Age at diagnosis	599	1.01 (1.00 – 1.01)	0.17	1.01 (1.00 – 1.01)	0.22	
Stage						
Early	29	Ref.	3.97×10^{-9}	Ref.	1.63×10^{-6}	
Advanced	570	3.43 (2.08 – 5.65)		2.91 (1.75 – 4.85)		
Debulking status						
<1 cm remaining	455	Ref.	7.50×10^{-6}	Ref.	1.95×10^{-4}	
>= 1 cm remaining	144	1.61 (1.32 – 1.97)		1.51 (1.22 – 1.86)		
Study site						
TCGA	259	Ref.	3.95×10^{-3}	Ref.	0.14	
Mayo Clinic	309	0.88 (0.73 – 1.06)		1.03 (0.85 – 1.24)		
AOCs	31	1.76 (1.19 – 2.60)		1.51 (1.02 – 2.25)		
TAP1 RNA expression	599	0.88 (0.82 – 0.94)	5.14×10^{-4}	1.00 (0.90 – 1.11)	1.00	
Gene expression molecular subtype						
C2.IMM	140	Ref.	6.15×10^{-3}	Ref.	0.25	
C1.MES	166	1.53 (1.19 – 1.96)		1.09 (0.83 – 1.43)		
C4.DIF	142	1.39 (1.07 – 1.80)		1.18 (0.89 – 1.55)		
C5.PRO	151	1.37 (1.06 – 1.78)		0.92 (0.67 – 1.25)		
Methylation signature	599	2.19 (1.74 – 2.76)	3.83×10^{-11}	2.22 (1.66 – 2.95)	4.46×10^{-8}	

HR, hazard ratio for time to event (recurrent/death) analysis risk for per-unit increase in methylation signature; p-value from likelihood ratio testing; TCGA, Mayo Clinic, AOCs; for age, results of univariate analyses are shown in the age-adjusted column.